International Journal of Heat and Mass Transfer 53 (2010) 3222–3230

Contents lists available at ScienceDirect

International Journal of Heat and Mass Transfer

journal homepage: www.elsevier.com/locate/ijhmt

A synthesis of tortuosity and dispersion in effective thermal conductivity of porous media

C. Yang [a,b], A. Nakayama [a,c,*]

[a] Department of Mechanical Engineering, Shizuoka University, 3-5-1 Johoku, Hamamatsu 432-8561, Japan
[b] School of Energy and Power Engineering, Huazhong University of Science and Technology, Wuhan, Hubei 430074, China
[c] Department of Civil Engineering, Wuhan Polytechnic University, Wuhan, Hubei 430023, China

ARTICLE INFO

Article history:
Received 7 October 2009
Received in revised form 19 January 2010
Accepted 19 February 2010
Available online 26 March 2010

Keywords:
Effective thermal conductivity
Porous media
Tortuosity
Dispersion

ABSTRACT

Effects of tortuosity and dispersion on the effective thermal conductivity of fluid-saturated porous media are investigated analytically with help of a volume averaging theory. Firstly, a general expression for the effective stagnant thermal conductivity has been derived using a unit cell model, which consists of rectangular solids with connecting arms in an in-line arrangement. The validity of the expression for the stagnant thermal conductivity has been confirmed comparing the present results with available experimental and theoretical data for packed beds, porous foams and wire screens. Secondly, an general expression for the thermal dispersion conductivity has been sought with help of the two energy equations for solid and fluid phases, derived on the basis of a volume averaging theory. It has been shown that the interstitial heat transfer between the solid and fluid phases is closely associated with the thermal dispersion. The resulting expressions for the longitudinal and transverse thermal dispersion conductivities agree well with available experimental data and empirical correlations.

1. Introduction

An effective thermal conductivity of a fluid-saturated porous medium is composed of stagnant thermal conductivity and thermal dispersion conductivity. For the case of pure heat conduction, the thermal dispersion conductivity is absent. In such heat conduction case, it is crucial to estimate the effects of tortuosity on the stagnant thermal conductivity, since the thermal conductivity of the solid phase is generally much higher than that of the fluid phase, and thus, whether the solid is connected or not influences the heat conduction mode significantly. Thermal dispersion, on the other hand, is the spreading of heat caused by variations in fluid velocity about the mean velocity. In addition to the molecular thermal diffusion, there is significant mechanical dispersion in heat and fluid flow in a fluid-saturated porous medium, as a result of hydrodynamic mixing of the fluid particles passing through pores. This thermal dispersion causes additional heat transfer, which arises further complications in dealing with transport processes in fluid-saturated porous media.

Accurate estimation of effective stagnant thermal conductivity of porous media has been continuously investigated since the pioneering work of Maxwell [1]. Standard treatment of heat conduction in porous media is based largely on the lumped mixture model under the assumption of local thermal equilibrium condition. In this treatment, the problem reduces to the construction of an appropriate composite model for the estimation of effective stagnant thermal conductivity. Such attempts include Rayleigh [2], Deissler and Boegli [3], Kunii and Smith [4], Zehner and Schlunder [5], Nozad et al. [6], Sahraouni and Kaviany [7] and Hsu et al. [8,9]. Hsu et al. [9] introduced a one-dimensional conduction model based on in-line touching cubes, and carried out an elegant analysis to show good agreement with the experimental data for the case of packed beds. As for consolidated porous media, Calmid and Mahajan [10,11] conducted a comprehensive study on the effective thermal conductivity of high porosity fibrous metal foams, introducing a one-dimensional heat conduction model. They found that their analysis agrees fairly well with the experimental data. Chang [12], on the other hand, developed a comparatively simple theoretical model based on combined series and parallel conduction within fluid saturated wire screens. He concluded that his analytical model provides better accuracy than the existing correlations. Excellent reviews on this topic may be found in Kaviany [13] and Hsu [14].

In the first part of this paper, we shall consider macroscopic heat conduction in porous media in a somewhat more general way by appealing to a volume averaging procedure [15–17]. We shall introduce a unit cell model, which consists of rectangular sol-

* Corresponding author. Address: Department of Mechanical Engineering, Shizuoka University, 3-5-1 Johoku, Hamamatsu 432-8561, Japan. Tel./fax: +81 53 478 1049.
E-mail address: tmanaka@ipc.shizuoka.ac.jp (A. Nakayama).

0017-9310/$ - see front matter © 2010 Elsevier Ltd. All rights reserved.
doi:10.1016/j.ijheatmasstransfer.2010.03.004

Nomenclature

A	surface area (m^2)
A_{int}	interface between the fluid and solid (m^2)
a_f	specific surface area (1/m)
c	specific heat (J/kg K)
c_p	specific heat at constant pressure (J/kg K)
C	size of the touching arm (m)
D	size of the solid (m)
F, f, g	profile functions (–)
H	size of the cell (m)
h_f	interfacial heat transfer coefficient (W/m^2 K)
k	thermal conductivity (W/m K)
L	external scale (m)
n_j	unit vector pointing outward from the fluid side to solid side (–)
Pr	Prandtl number (–)
q	heat flux (W/m^2)
$R_{a,b,c,f,s}$	thermal resistances
T	temperature (K)
V	representative elementary volume (m^3)
x_i	Cartesian coordinates (m)
x, y, z	Cartesian coordinates (m)
ε	porosity (–)
η	dimensionless vertical coordinate (–)
ρ	density (kg/m^3)

Special symbols

$\tilde{\phi}$	deviation from intrinsic average
$\langle\phi\rangle$	Darcian average
$\langle\phi\rangle^{f,s}$	intrinsic average

Subscripts and superscripts

f	fluid
s	solid

ids with connecting arms in an in-line arrangement. This general model allows us to represent most homogeneous porous media, which may or may not have directional dependence. Packed beds, porous foams and wire screens may easily be described by setting geometrical parameters in the model accordingly. The terms associated with the tortuosity in porous media are evaluated, by faithfully carrying out surface integrations with respect to the local temperature over the interface between the solid and fluid phases.

In the second part of this paper, we shall investigate the thermal dispersion conductivity, which becomes predominant for convective flows in porous media. According to Wakao and Kaguei [18], Yagi et al. [19] were the first to measure the effective longitudinal thermal conductivities of packed bed, taking full account of the effect of thermal dispersion, and eventually found the longitudinal component of the dispersion coefficient much greater than its transverse component. Since the famous analytical treatment in a tube by Taylor [20], a number of theoretical and experimental efforts (e.g. Aris [21], Koch and Brady [22], Han et al. [23] and Vortmeyer [24]) were made to establish useful correlations for estimating the effective thermal conductivities due to thermal dispersion (see Kaviany [13]). Furthermore, a series of numerical experiments were conducted by Kuwahara et al. [25] and Kuwahara and Nakayama [26], assuming a macroscopically uniform flow through a lattice of rods, so as to elucidate the effects of microscopic velocity and temperature fields on the thermal dispersion. It is also worthwhile to mention that Nakayama et al. [27] derived a thermal dispersion heat flux transport equation from the volume averaged version of Navier–Stokes and energy equations and showed that it naturally reduces to an algebraic expression for the effective thermal conductivity based on a gradient-type diffusion hypothesis.

In this paper, we shall revisit the volume average version of the two energy equations for solid and fluid phases, derived on the basis of the volume averaging theory [28]. We shall follow the definition of thermal dispersion heat flux to evaluate the longitudinal and transverse components of the thermal dispersion conductivity, exploiting the derived two energy equations. It will be shown that the interstitial heat transfer is closely linked with the thermal dispersion phenomena. A general expression will be derived using the inter-relationship found between the interstitial heat transfer and thermal dispersion. The validity of general expressions for both stagnant thermal conductivity and thermal dispersion conductivity will be confirmed comparing the present results with available experimental and theoretical data.

2. Macroscopic energy equations

We shall consider the energy equation for the fluid phase and that for the solid matrix phase as follows:

For the fluid phase:

$$\rho_f c_{p_f}\frac{\partial T}{\partial t}+\rho_f c_{p_f}\frac{\partial}{\partial x_j}u_j T=\frac{\partial}{\partial x_j}\left(k_f\frac{\partial T}{\partial x_j}\right) \tag{1}$$

For the matrix phase:

$$\rho_s c_s\frac{\partial T}{\partial t}=\frac{\partial}{\partial x_j}\left(k_s\frac{\partial T}{\partial x_j}\right) \tag{2}$$

where the subscripts f and s stand for the fluid phase and solid phase, respectively. In order to obtain the macroscopic energy equation for fluid-saturated porous media, we take a control volume V within in the medium, whose length scale $V^{1/3}$ is much smaller than the macroscopic characteristic length, but, at the same time, much greater than the structural characteristic length (see e.g. Nakayama [15]). Under this condition, the volume average of a certain variable ϕ in the fluid phase is defined as

$$\langle\phi\rangle^f\equiv\frac{1}{V_f}\int_{V_f}\phi\,dV \tag{3}$$

where V_f is the volume space which the fluid phase occupies. The porosity $\varepsilon\equiv V_f/V$ is the volume fraction of the fluid space. Following Nakayama [15], Cheng [16], Quintard and Whitaker [17] and many others, we decompose a variable ϕ into its intrinsic average and the spatial deviation from it:

$$\phi=\langle\phi\rangle^f+\tilde{\phi} \tag{4}$$

We shall exploit the following spatial average relationships:

$$\langle\phi_1\phi_2\rangle^f=\langle\phi_1\rangle^f\langle\phi_2\rangle^f+\langle\tilde{\phi}_1\tilde{\phi}_2\rangle^f \tag{5}$$

$$\left\langle\frac{\partial\phi}{\partial x_i}\right\rangle^f=\frac{1}{\varepsilon}\frac{\partial\varepsilon\langle\phi\rangle^f}{\partial x_i}+\frac{1}{V_f}\int_{A_{int}}\phi n_i\,dA \tag{6}$$

where A_{int} is the local interfacial area between the fluid and solid matrix, while n_i is the unit vector pointing outward from the fluid side to solid side. Similar relationships hold for the solid phase, whose intrinsic average is defined as

$$\langle\phi\rangle^s\equiv\frac{1}{V_s}\int_{V_s}\phi\,dV \tag{7}$$

Upon integrating Eqs. (1) and (2) over the local control volume with help of the foregoing relationships, we obtain the volume averaged set of the energy equations as follows [28]:

For the fluid phase:

$$\rho_f c_{p_f}\varepsilon\frac{\partial\langle T\rangle^f}{\partial t}+\rho_f c_{p_f}\varepsilon\frac{\partial\langle u_j\rangle^f\langle T\rangle^f}{\partial x_j} =\frac{\partial}{\partial x_j}\left(\varepsilon k_f\frac{\partial\langle T\rangle^f}{\partial x_j}+\frac{k_f}{V}\int_{A_{int}}Tn_j\,dA-\rho_f c_{p_f}\varepsilon\langle\tilde{u}\tilde{T}\rangle^f\right) +\frac{1}{V}\int_{A_{int}}k_f\frac{\partial T}{\partial x_j}n_j\,dA \tag{8}$$

For the solid matrix phase:

$$\rho_s c_s(1-\varepsilon)\frac{\partial\langle T\rangle^s}{\partial t}=\frac{\partial}{\partial x_j}\left((1-\varepsilon)k_s\frac{\partial\langle T\rangle^s}{\partial x_j}-\frac{k_s}{V}\int_{A_{int}}Tn_j\,dA\right) -\frac{1}{V}\int_{A_{int}}k_f\frac{\partial T}{\partial x_j}n_j\,dA \tag{9}$$

where $\langle T\rangle^f$ is the intrinsic average of the fluid temperature, while $\langle T\rangle^s$ is the intrinsic average of the solid matrix temperature. Obviously, the parenthetical terms on the right hand side of Eq. (8) denote the diffusive heat transfer, while the last term describes the interfacial heat transfer between the solid and fluid phases. We combine the foregoing two energy equations to obtain a single macroscopic equation as follows:

$$\frac{\partial(\varepsilon\rho_f c_{p_f}\langle T\rangle^f+(1-\varepsilon)\rho_s c_s\langle T\rangle^s)}{\partial t}+\varepsilon\rho_f c_{p_f}\frac{\partial\langle u_j\rangle^f\langle T\rangle^f}{\partial x_j} =\frac{\partial}{\partial x_j}\left(\varepsilon k_f\frac{\partial\langle T\rangle^f}{\partial x_j}+(1-\varepsilon)k_s\frac{\partial\langle T\rangle^s}{\partial x_j}+\frac{k_f-k_s}{V}\int_{A_{int}}Tn_j\,dA-\varepsilon\rho_f c_{p_f}\langle\tilde{u}\tilde{T}\rangle^f\right) \tag{10}$$

where we exploited the continuity of temperature and heat flux at the interface. Further assuming that the local thermal equilibrium condition holds between both phases, namely, $\langle T\rangle^f=\langle T\rangle^s=\langle T\rangle$, the equation reduces to

$$(\varepsilon\rho_f c_{p_f}+(1-\varepsilon)\rho_s c_s)\frac{\partial\langle T\rangle}{\partial t}+\rho_f c_{p_f}\frac{\partial\langle u_j\rangle\langle T\rangle}{\partial x_j} =\frac{\partial}{\partial x_j}\left((\varepsilon k_f+(1-\varepsilon)k_s)\frac{\partial\langle T\rangle}{\partial x_j}+\frac{k_f-k_s}{V}\int_{A_{int}}Tn_j\,dA-\varepsilon\rho_f c_{p_f}\langle\tilde{u}_j\tilde{T}\rangle^f\right) \tag{11}$$

where

$$\langle\phi\rangle\equiv\frac{1}{V}\int_V\phi\,dV \tag{12}$$

is the Darcian average of the variable ϕ such that $\langle u_j\rangle=\varepsilon\langle u_j\rangle^f$ is the Darcian velocity vector. Thus, we find the macroscopic heat flux vector q_j and its corresponding total effective thermal conductivity tensor $k_{total_{ij}}$ as follows:

$$q_i=-k_{total_{ij}}\frac{\partial\langle T\rangle}{\partial x_j} =-(\varepsilon k_f+(1-\varepsilon)k_s)\frac{\partial\langle T\rangle}{\partial x_i}-(k_f-k_s)\left\langle\frac{1}{V}\int_{A_{int}}Tn_i\,dA\right\rangle+\varepsilon\rho_f c_{p_f}\langle\tilde{u}_i\tilde{T}\rangle^f \tag{13}$$

The last term in the rightmost expression describes the thermal dispersion term, while the second associated with the surface integral describes the effects of the tortuosity on the macroscopic heat flux. Note that the first term in the expression corresponds to the upper bound of the effective stagnant thermal conductivity based on the parallel model, namely, $(\varepsilon k_f+(1-\varepsilon)k_s)\delta_{ij}$. Thus, it is the tortuosity term (i.e. the second term) that adjusts the level of the effective stagnant thermal conductivity from its upper bound to a correct one.

3. Unit cell model and effective stagnant thermal conductivity

The present unit cell model of rectangular solid is illustrated in Fig. 1. We assume that an infinite number of these rectangular solids are arranged in a regular fashion. The dimensions of the unit cell and rectangular solid are indicated as $(H_x,\ H_y,\ H_z)$ and $(D_x,\ D_y,\ D_z)$, respectively, while the sizes of touching arms of square crosssection are denoted by $(C_x,\ C_y,\ C_z)$, respectively.

We shall apply Eq. (13) to this unit model so as to find out the effective stagnant thermal conductivity. The axial component of the surface integral term in the second term in the rightmost expression in Eq. (13) may be estimated as follows:

$$\begin{aligned}\vec{i}\cdot\left\langle\frac{1}{V}\int_{A_{int}}Tn_i\,dA\right\rangle&=\vec{i}\cdot\frac{1}{H_xH_yH_z}\int_0^{H_z}\int_0^{H_y}\int_0^{H_x}\left(\frac{1}{V(x,y,z)}\int_{A_{int}}Tn_i\,dA\right)dxdydz\\ &=\int_{D_yD_z-C_x^2}\left(T|_{x=-\frac{D_x}{2}}-T|_{x=\frac{D_x}{2}}\right)dA\Big|_{C.V.1}\frac{H_x-D_x}{H_x^2H_yH_z}\\ &\quad-\int_{D_yD_z-C_x^2}\left(T|_{x=\frac{D_x}{2}}-T|_{x=-\frac{D_x}{2}+H_x}\right)dA\Big|_{C.V.2}\frac{D_x}{H_x^2H_yH_z}\\ &\quad+\int_{C_y(H_y-D_y)}\left(T|_{x=-\frac{C_y}{2}}-T|_{x=\frac{C_y}{2}}\right)dA\Big|_{C.V.1}\frac{H_x-C_y}{H_x^2H_yH_z}\\ &\quad-\int_{C_y(H_y-D_y)}\left(T|_{x=\frac{C_y}{2}}-T|_{x=-\frac{C_y}{2}+H_x}\right)dA\Big|_{C.V.2}\frac{C_y}{H_x^2H_yH_z}\\ &\quad+\int_{C_z(H_z-D_z)}\left(T|_{x=-\frac{C_z}{2}}-T|_{x=\frac{C_z}{2}}\right)dA\Big|_{C.V.1}\frac{H_x-C_z}{H_x^2H_yH_z}\\ &\quad-\int_{C_z(H_z-D_z)}\left(T|_{x=\frac{C_z}{2}}-T|_{x=-\frac{C_z}{2}+H_x}\right)dA\Big|_{C.V.2}\frac{C_z}{H_x^2H_yH_z}\end{aligned} \tag{14}$$

Upon noting that n_i is the unit vector pointing outward from the fluid side to solid side, we considered the two distinctive control volumes, namely, *C.V.1* and *C.V.2*, as shown in Fig. 2, with their corresponding weights, to evaluate the volume average of the surface integral term associated with the interfacial temperatures.

The temperature differences between the opposing interfaces may be estimated considering the heat currents, namely,

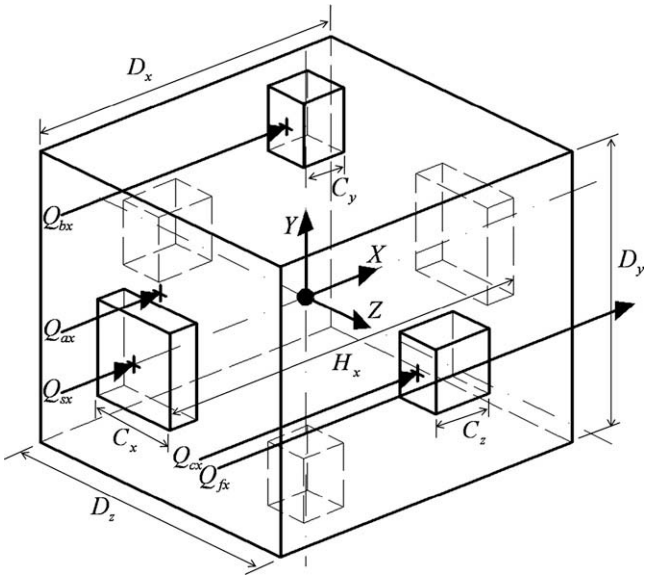

Fig. 1. Unit cell model.

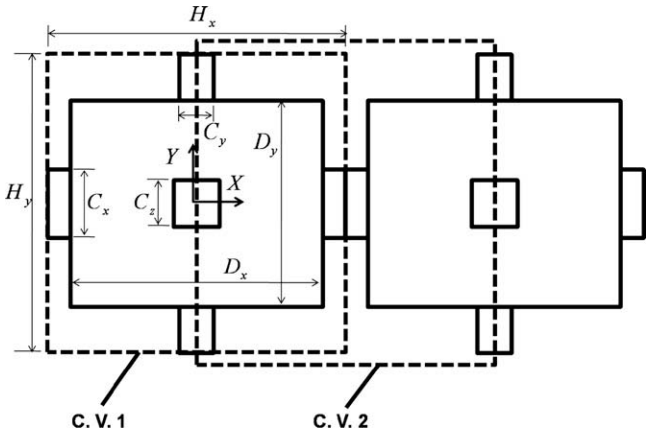

Fig. 2. Two distinctive control volumes for the surface integral.

Q_{a_x}, Q_{b_x}, Q_{c_x}, Q_{s_x} and Q_{f_x}, as indicated in Fig. 1, and their corresponding thermal circuits as shown in Fig. 3, such that

$$\left(T|_{x=-\frac{D_x}{2}} - T|_{x=\frac{D_x}{2}}\right) = \frac{Q_{a_x} D_x}{(D_y D_z - C_x^2)k_s} = \frac{\frac{1}{R_{a_x}} q_x H_y H_z D_x}{\left(\frac{1}{R_{a_x}} + \frac{1}{R_{s_x}} + \frac{1}{R_{b_x}} + \frac{1}{R_{c_x}} + \frac{1}{R_{f_x}}\right)(D_y D_z - C_x^2)k_s} \tag{15}$$

where

$$R_{a_x} = \left(\frac{H_x - D_x}{k_f} + \frac{D_x}{k_s}\right)\frac{1}{D_y D_z - C_x^2} \tag{16a}$$

$$R_{s_x} = \frac{H_x}{k_s C_x^2} \tag{16b}$$

$$R_{b_x} = \left(\frac{H_x - C_y}{k_f} + \frac{C_y}{k_s}\right)\frac{1}{C_y(H_y - D_y)} \tag{16c}$$

$$R_{c_x} = \left(\frac{H_x - C_z}{k_f} + \frac{C_z}{k_s}\right)\frac{1}{C_z(H_z - D_z)} \tag{16d}$$

$$R_{f_x} = \frac{H_x}{k_f}\frac{1}{H_y H_z - D_y D_z - C_y(H_y - D_y) - C_z(H_z - D_z)} \tag{16e}$$

The other temperature differences may be evaluated likewise.

Substituting these temperature differences into Eq. (14), we find

$$\vec{i}\cdot\left\langle \frac{1}{V}\int_{A_{int}} T n_i dA\right\rangle = \vec{i}\cdot\frac{1}{H_x H_y H_x}\int_0^{H_z}\int_0^{H_y}\int_0^{H_x}\left(\frac{1}{V(x,y,z)}\int_{A_{int}} T n_i dA\right)dxdydz$$
$$= \frac{\frac{1}{R_{a_x}}}{\frac{1}{R_{a_x}} + \frac{1}{R_{s_x}} + \frac{1}{R_{b_x}} + \frac{1}{R_{c_x}} + \frac{1}{R_{f_x}}} q_x\left(\frac{1}{k_s} - \frac{1}{k_f}\right)\frac{(H_x - D_x)D_x}{H_x^2}$$
$$+ \frac{\frac{1}{R_{b_x}}}{\frac{1}{R_{a_x}} + \frac{1}{R_{s_x}} + \frac{1}{R_{b_x}} + \frac{1}{R_{c_x}} + \frac{1}{R_{f_x}}} q_x\left(\frac{1}{k_s} - \frac{1}{k_f}\right)\frac{(H_x - C_y)C_y}{H_x^2}$$
$$+ \frac{\frac{1}{R_{c_x}}}{\frac{1}{R_{a_x}} + \frac{1}{R_{s_x}} + \frac{1}{R_{b_x}} + \frac{1}{R_{c_x}} + \frac{1}{R_{f_x}}} q_x\left(\frac{1}{k_s} - \frac{1}{k_f}\right)\frac{(H_x - C_z)C_z}{H_x^2} \tag{17}$$

The foregoing expressions are substituted into the definition of the macroscopic heat flux, namely, Eq. (13) without the dispersion term, to find

$$q_x = -k_{stag_{xx}}\frac{\partial\langle T\rangle}{\partial x} = -(\varepsilon k_f + (1-\varepsilon)k_s)\frac{\partial\langle T\rangle}{\partial x} - \frac{(k_f - k_s)\left(\frac{1}{k_s} - \frac{1}{k_f}\right)q_x}{\left(\frac{1}{R_{a_x}} + \frac{1}{R_{s_x}} + \frac{1}{R_{b_x}} + \frac{1}{R_{c_x}} + \frac{1}{R_{f_x}}\right)} \times\left(\frac{1}{R_{a_x}}\left(1 - \frac{D_x}{H_x}\right)\frac{D_x}{H_x} + \frac{1}{R_{b_x}}\left(1 - \frac{C_y}{H_x}\right)\frac{C_y}{H_x} + \frac{1}{R_{c_x}}\left(1 - \frac{C_z}{H_x}\right)\frac{C_z}{H_x}\right) \tag{18}$$

Upon solving for the macroscopic heat flux q_x, we have

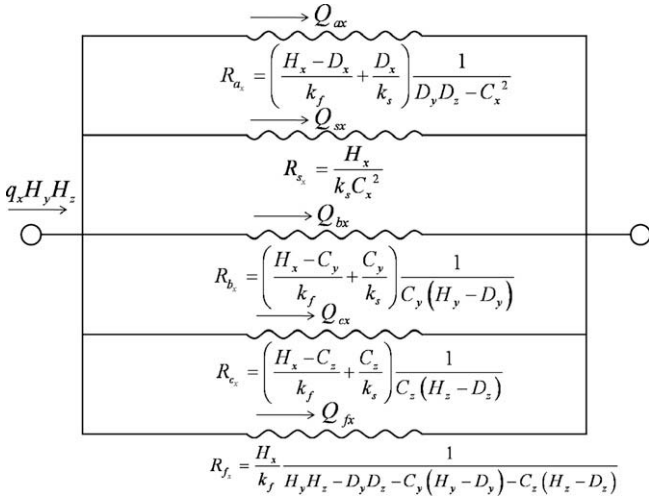

Fig. 3. Thermal circuit.

$$q_x = -k_{stag_{xx}}\frac{\partial\langle T\rangle}{\partial x} = -\frac{\varepsilon k_f + (1-\varepsilon)k_s}{1 + \frac{(k_f - k_s)^2}{k_s k_f}\frac{\frac{1}{R_{a_x}}\left(1 - \frac{D_x}{H_x}\right)\frac{D_x}{H_x} + \frac{1}{R_{b_x}}\left(1 - \frac{C_y}{H_x}\right)\frac{C_y}{H_x} + \frac{1}{R_{c_x}}\left(1 - \frac{C_z}{H_x}\right)\frac{C_z}{H_x}}{\frac{1}{R_{a_x}} + \frac{1}{R_{s_x}} + \frac{1}{R_{b_x}} + \frac{1}{R_{c_x}} + \frac{1}{R_{f_x}}}}\frac{\partial\langle T\rangle}{\partial x} \tag{19}$$

which gives the effective stagnant thermal conductivity as follows:

$$k_{stag_{xx}} = \frac{\varepsilon k_f + (1-\varepsilon)k_s}{1 + \frac{(k_f - k_s)^2}{k_s k_f}\frac{\frac{1}{R_{a_x}}\left(1 - \frac{D_x}{H_x}\right)\frac{D_x}{H_x} + \frac{1}{R_{b_x}}\left(1 - \frac{C_y}{H_x}\right)\frac{C_y}{H_x} + \frac{1}{R_{c_x}}\left(1 - \frac{C_z}{H_x}\right)\frac{C_z}{H_x}}{\frac{1}{R_{a_x}} + \frac{1}{R_{s_x}} + \frac{1}{R_{b_x}} + \frac{1}{R_{c_x}} + \frac{1}{R_{f_x}}}} \tag{20a}$$

Likewise,

$$k_{stag_{yy}} = \frac{\varepsilon k_f + (1-\varepsilon)k_s}{1 + \frac{(k_f - k_s)^2}{k_s k_f}\frac{\frac{1}{R_{a_y}}\left(1 - \frac{D_y}{H_y}\right)\frac{D_y}{H_y} + \frac{1}{R_{b_y}}\left(1 - \frac{C_z}{H_y}\right)\frac{C_z}{H_y} + \frac{1}{R_{c_y}}\left(1 - \frac{C_x}{H_y}\right)\frac{C_x}{H_y}}{\frac{1}{R_{a_y}} + \frac{1}{R_{s_y}} + \frac{1}{R_{b_y}} + \frac{1}{R_{c_y}} + \frac{1}{R_{f_y}}}} \tag{20b}$$

$$k_{stag_{zz}} = \frac{\varepsilon k_f + (1-\varepsilon)k_s}{1 + \frac{(k_f - k_s)^2}{k_s k_f}\frac{\frac{1}{R_{a_z}}\left(1 - \frac{D_z}{H_z}\right)\frac{D_z}{H_z} + \frac{1}{R_{b_z}}\left(1 - \frac{C_x}{H_z}\right)\frac{C_x}{H_z} + \frac{1}{R_{c_z}}\left(1 - \frac{C_y}{H_z}\right)\frac{C_y}{H_z}}{\frac{1}{R_{a_z}} + \frac{1}{R_{s_z}} + \frac{1}{R_{b_z}} + \frac{1}{R_{c_z}} + \frac{1}{R_{f_z}}}} \tag{20c}$$

The set of Eq. (16) should be used with cyclic permutation to obtain the resistances R_{a_y} to R_{f_z} in Eqs. (20b) and (20c). Moreover, the porosity of the unit cell of rectangular solid may be evaluated from

$$\varepsilon = \frac{H_x H_y H_z - D_x D_y D_z - C_x^2(H_x - D_x) - C_y^2(H_y - D_y) - C_z^2(H_z - D_z)}{H_x H_y H_z} \tag{21}$$

4. Validation of the expression for stagnant thermal conductivity

In order to examine the generality acquired in our mathematical model for estimating the effective stagnant thermal conductivity, we shall apply our model to evaluate the effective stagnant thermal conductivities of various porous media, such as packed beds, metal foams and wire screens.

4.1. Packed beds

Hsu et al. [9] introduced a unit cell model of touching cubes in a regular arrangement and carried out a lumped mixture model analysis and predicted the effective stagnant thermal conductivity of the packed beds. They showed that their model of cubes in a regular arrangement is a rational model to describe heat transfer in

the packed beds. Albeit the difference in its appearance, our general expression based on the volume averaging theory, when applied to their geometry, turns out to be mathematically identical to their expression based on the lumped mixture model. Thus, as for the first example, we shall predict the effective stagnant thermal conductivity of the packed beds. The geometrical parameters for the packed beds may be set following Hsu et al. [9]:

$$H_x = H_y = H_z = H, \quad D_x = D_y = D_z = D,$$
$$C_x = C_y = C_z = C = 0.13D \tag{22a}$$

$$\varepsilon = 1 - \left(\frac{D}{H}\right)^3 - 3 \times 0.13^2 \left(\frac{D}{H}\right)^2 \left(1 - \frac{D}{H}\right) = 0.36 \tag{22b}$$

We have approximated the collection of the spherical particles in the packed bed by the collection of the cubes with touching arms of square cross section. Note that its porosity ($\varepsilon = 0.36$) is set to the same as that of their packed beds. Eq. (22a) together with (22b) gives

$$D/H = 0.86 \quad \text{and} \quad C/H = 0.11 \tag{23}$$

As we substitute foregoing values into Eq. (20a), the ratio of the effective stagnant thermal conductivity $k_{stag_{xx}}/k_f$ may readily be evaluated for each value of the solid to fluid thermal conductivity ratio, k_s/k_f. Such a curve showing $k_{stag_{xx}}/k_f$ is generated from Eq. (20a) and plotted in Fig. 4 along with the experimental data of Nozad et al. [6] for the case of the packed beds. The prediction follows the experimental data closely over a wide range of the thermal conductivity ratio. Note that the size ratio of the touching arm to the rectangular solid, namely, C/D, accounts for the contact resistance between the particles. Naturally, the resulting stagnant thermal conductivity is fairly sensitive to the ratio C/D. Empirical information on the contact resistance is needed to set the ratio.

4.2. Metal foams

Our general set of Eqs. (20) can also be used for evaluating the effective stagnant thermal conductivities of high porosity metal foams. In reality, the structure of metal foams is quite complex. Therefore, it may not be practical to describe all details of the structure accurately. Calmid and Mahajan [10] approximated such a complex structure, introducing a hexagonal structure of metal foam matrix. In this way, they were able to obtain the expression for the effective stagnant thermal conductivity exploiting a one-dimensional heat conduction concept. Their prediction agrees very well with available experimental data. Alternatively, we may apply our general model to high porosity metal foams, by setting the geometrical parameters as

$$H_x = H_y = H_z = H, \quad D_x = D_y = D_z = C_x = C_y = C_z = D \tag{24a}$$

$$\varepsilon = 1 - 3\left(\frac{D}{H}\right)^2 + 2\left(\frac{D}{H}\right)^3 \tag{24b}$$

Note that the metal foam structure was approximated by a unit cubic cell structure according to Eq. (24a), and that the porosity was set equal to that of the corresponding metal form. Eq. (24b) for the porosity of the unit cubic cell may readily be derived as we subtract the square rod volume per unit $(3(H-D)D^2 + D^3)$ from the unit volume H^3 to obtain the space occupied by the fluid per unit cell, then divided it by H^3.

In Fig. 5, our prediction based on Eq. (20a) is shown along with Calmid–Mahajan expression based their hexagonal model [10] for $k_s/k_f = 357$ and 8226, over the porosity range from 0.90 to 0.98. As can be seen from the figure, both predictions agree with the experimental data very well.

4.3. Wire screens

As for the third example, we shall consider wire screens and apply our general model to estimate their effective stagnant thermal conductivities. A multiple layer of square-mesh standard wire screens is depicted in Fig. 6.

The multiple layers of wire screens of this kind are often used for heat pipe applications. Thus, it is essential to estimate the effective thermal conductivity of wire screens, as we use them for various heat transfer applications. Chang [12] proposed a comparatively simple theoretical model based on combined series and parallel conduction and showed that his equation gives fairly good agreement with available experimental data. Our general Eq. (20a) may also be applied for this case, in order to estimate the effective thermal conductivity of the multiple layers of wire screens. A careful observation of the cross section of the wire screen, as shown in Fig. 6 prompts us to set the geometrical parameters as follows:

$$H_x = H_y = H_z = H, \quad D_x/2 = D_y = D_z = D,$$
$$C_x = 0.032D, \quad C_y = D, \quad C_z = D \tag{25a}$$

$$\varepsilon = 1 - 2\left(\frac{D}{H}\right)^3 - 0.032^2 \left(\frac{D}{H}\right)^2 \left(1 - 2\frac{D}{H}\right) - 2\left(\frac{D}{H}\right)^2 \left(1 - \frac{D}{H}\right) = 0.70 \tag{25b}$$

such that $D/H = 0.39$. We estimated the touching area as $C_x = 0.032D$ for a multiple layers of wire screens.

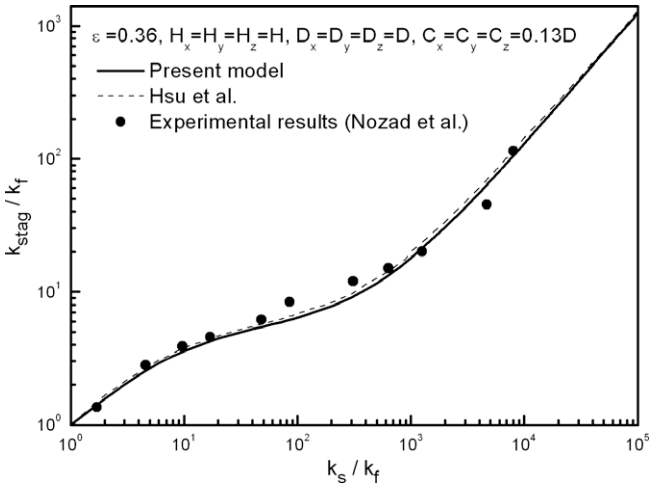

Fig. 4. Effective stagnant thermal conductivity of packed beds.

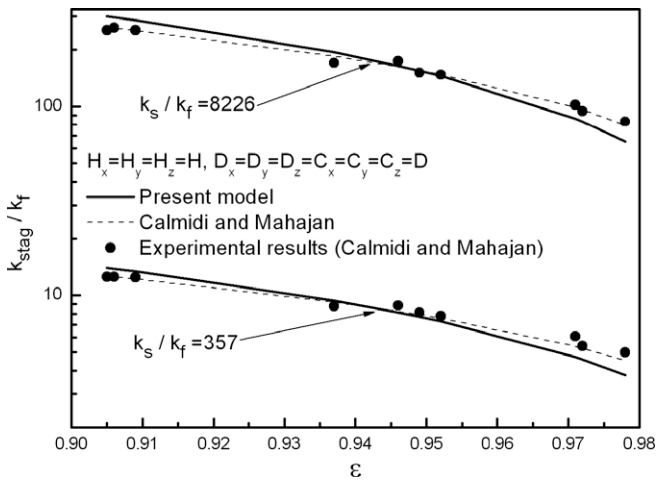

Fig. 5. Effective stagnant thermal conductivity of metal foams.

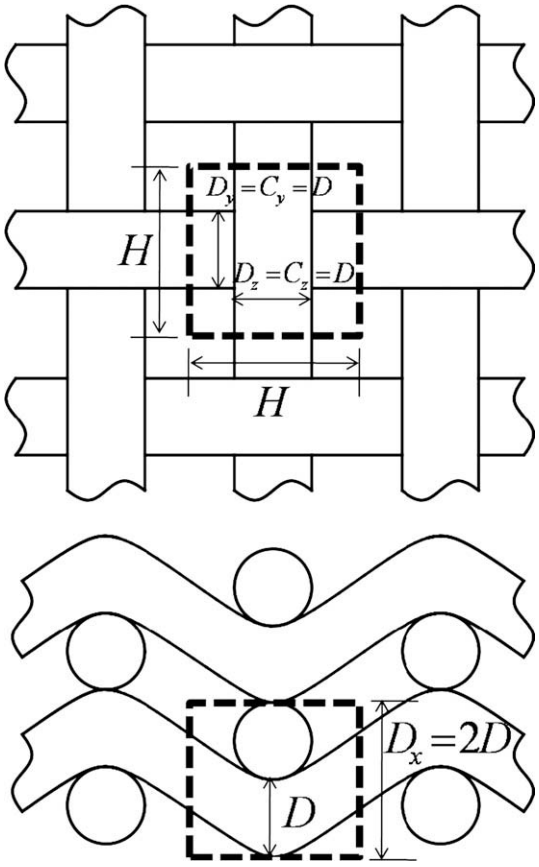

Fig. 6. Schematic views of wire screens.

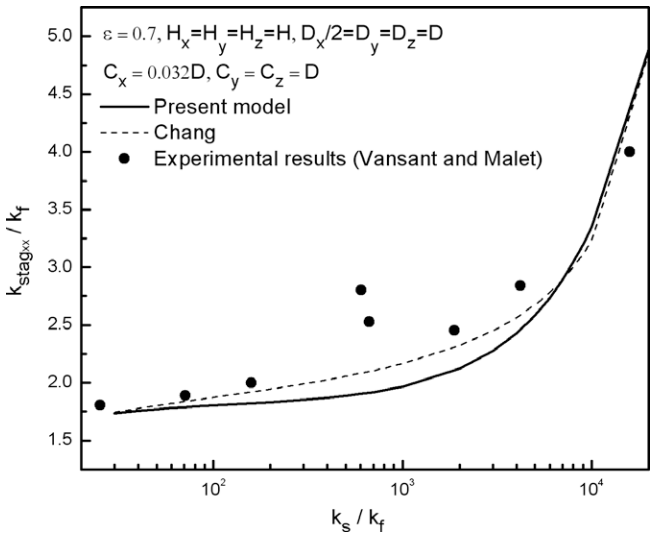

Fig. 7. Effective stagnant thermal conductivity of a multiple layer of wire screens.

Note that the wire screen structure was approximated by a unit cell structure of a rectangular prism $2D \times D \times D$ with four thick arms $D \times D \times (H-D)/2$ and two thin arms $0.032D \times 0.032D \times (H-2D)/2$ as given by Eq. (25a), and that the porosity was set equal to that of the corresponding wire screens. Eq. (25b) for the porosity of the unit cell may be derived as we subtract the solid volume per unit $2D^3 + 0.032^2D^2(H-2D) + 2D^2(H-D)$ from the unit volume H^3 to obtain the space occupied by the fluid per unit cell, then divided it by H^3.

Our prediction based on the general Eq. (20a) is illustrated in Fig. 7, which indicates fairly good agreement among our prediction, Chang's prediction and the experimental data of the wire screens reported by VanSant and Malet [29]. This suggests that our general set of Eqs. (20) is valid even for the prediction of effective stagnant thermal conductivity tensors in anisotropic porous media.

5. Expressions for thermal dispersion conductivity

Even when the local thermal equilibrium holds at the macroscopic scale, the interstitial heat transfer takes place between the solid and fluid phases. In other words, the interface at the pore scale is never at local thermal equilibrium. In fact, it is this interfacial heat transfer at the local non-thermal equilibrium that controls the spatial distribution of the temperature at the pore scale and thus the thermal dispersion activities.

Upon introducing the interstitial heat transfer coefficient h_f and the effective porosity tensor, ε^*_{ij}, as function of the stagnant thermal conductivity tensor, $k_{stag_{ij}} = k_{stag_{xx}}(\overleftarrow{i},\vec{i}) + k_{stag_{yy}}(\vec{j},\vec{j}) + k_{stag_{zz}}(\vec{k},\vec{k})$, the two energy equations (8) and (9) may be rewritten, as follows:

For the fluid phase:

$$\rho_f c_{p_f} \varepsilon \frac{\partial \langle T\rangle^f}{\partial t} + \rho_f c_{p_f} \frac{\partial \langle u_j\rangle \langle T\rangle^f}{\partial x_j} = \frac{\partial}{\partial x_j}\left(\varepsilon^*_{jk} k_f + \varepsilon k_{dis_{jk}}\right)\frac{\partial \langle T\rangle^f}{\partial x_k} - a_f h_f\left(\langle T\rangle^f - \langle T\rangle^s\right) \tag{26}$$

For the solid matrix phase:

$$\rho_f c_{p_f}(1-\varepsilon)\frac{\partial \langle T\rangle^s}{\partial t} = \frac{\partial}{\partial x_j}\left((\delta_{jk} - \varepsilon^*_{jk})k_s \frac{\partial \langle T\rangle^s}{\partial x_k}\right) - a_f h_f(\langle T\rangle^s - \langle T\rangle^f) \tag{27}$$

where the effective porosity tensor is defined as

$$\varepsilon^*_{jk} = \varepsilon\delta_{jk} + \frac{(\varepsilon k_f + (1-\varepsilon)k_s)\delta_{jk} - k_{stag_{jk}}}{k_s - k_f} \tag{28}$$

such that $\varepsilon^*_{jk}k_f + (\delta_{jk} - \varepsilon^*_{jk})k_s = k_{stag_{jk}}$, while the dispersion thermal conductivity tensor is defined by

$$-\rho_f c_{p_f}\langle \tilde{u}_j \tilde{T}\rangle^f = k_{dis_{kj}}\frac{\partial \langle T\rangle^f}{\partial x_k} \tag{29}$$

Moreover, the interstitial heat transfer between the fluid and solid phases is modeled according to Newton's cooling law as

$$\frac{1}{V}\int_{A_{int}} k_f \frac{\partial T}{\partial x_j} n_j \, dA = -a_f h_f\left(\langle T\rangle^f - \langle T\rangle^s\right) \tag{30}$$

where a_f and h_f are the specific surface area and interfacial heat transfer coefficient, respectively.

5.1. Longitudinal thermal dispersion conductivity

The energy Eq. (26) at the steady state may be written along the macroscopic flow direction x as follows:

$$\rho_f c_{p_f}\langle u\rangle \frac{\partial \langle T\rangle^f}{\partial x} = -a_f h_f(\langle T\rangle^f - \langle T\rangle^s) \tag{31}$$

We have dropped the diffusion term, since the convection term on the left hand side predominates over the diffusion term, as the thermal dispersion becomes appreciable. A magnitude analysis reveals that the diffusive term in Eq. (26) may be neglected when the Peclet number based on an external scale L and dispersion thermal conductivity k_{dis}, namely, $\rho_f c_{p_f}\langle u\rangle L/k_{dis}$, is sufficiently large. As will be shown later (see Eq. (46)), we have $k_{dis} \sim \rho_f c_{p_f}\langle u\rangle D$ for convective

flows. Hence, $\rho_f c_{p_f}\langle u\rangle L/k_{dis} \sim L/D \gg 1$ and Eq. (31) may readily be satisfied for most convective flow cases. Exploiting the foregoing equation, the longitudinal thermal dispersion term may be evaluated as follows:

$$-\rho_f c_{p_f}\langle \tilde{u}\tilde{T}\rangle^f = -\rho_f c_{p_f}\langle u\rangle^f(\langle T\rangle^f - \langle T\rangle^s)\langle (f-1)(g-1)\rangle^f = \frac{(\rho_f c_{p_f}\langle u\rangle)^2}{\varepsilon a_f h_f}\langle (f-1)(g-1)\rangle^f \frac{\partial \langle T\rangle^f}{\partial x} \tag{32}$$

Hence,

$$k_{dis_{xx}} = \frac{(\rho_f c_{p_f}\langle u\rangle)^2}{\varepsilon a_f h_f}\langle (f-1)(g-1)\rangle^f \tag{33}$$

where

$$u = \langle u\rangle^f f(\eta) \tag{34a}$$

and

$$T - \langle T\rangle^s = (\langle T\rangle^f - \langle T\rangle^s) g(\eta) \tag{34b}$$

We shall consider a convective flow through cubes in a regular arrangement as shown in Fig. 8, where the dimensionless coordinate η is defined as

$$\eta = 2y/(H-D) \tag{35}$$

The cubes are assumed to have no touching arms, since the effects of such arms on the thermal dispersion may be negligibly small for packed beds of our interest. For the first approximation, we may assume the following profile functions describing the laminar fully developed velocity and temperature profiles:

$$f(\eta) = \frac{3}{2}(1-\eta^2) \tag{36a}$$

and

$$g(\eta) = \frac{5}{16}(5 - 6\eta^2 + \eta^4) \tag{36b}$$

Noting that $\langle \phi\rangle^f = \frac{1}{2}\int_{-1}^{1}\phi d\eta$ such that $\langle f\rangle^f = \langle g\rangle^f = 1$, and substituting the foregoing profiles into (33), we readily obtain

$$\frac{k_{dis_{xx}}}{k_f} = \frac{3}{14}\frac{(\rho_f c_{p_f}\langle u\rangle)^2}{\varepsilon a_f h_f k_f} = \frac{1}{28\varepsilon(1-\varepsilon)}\frac{Pe_D^2}{\left(\frac{h_f D}{k_f}\right)} \tag{37}$$

where $Pe_D = \rho_f c_{pf}\langle u\rangle D/k_f$ is Peclet number based on the Darcian velocity and particle diameter. Note also $a_f = 6(1-\varepsilon)/D$ for spherical particles of size D. Assuming $\varepsilon = 0.4$ and using Wakao and Kaguei's empirical equation [18] for the interstitial heat transfer coefficient for packed beds, namely,

$$\frac{h_f D}{k_f} = 2.0 + 1.1 Pe_D^{0.6}/Pr^{0.27} \tag{38}$$

we obtain the longitudinal thermal dispersion in the laminar regime as follows:

$$\frac{k_{dis_{xx}}}{k_f} = 0.15\frac{Pe_D^2}{2.0 + 1.1 Pe_D^{0.6}/Pr^{0.27}}: \quad \text{Laminar regime} \tag{39}$$

The foregoing equation gives $k_{dis_{xx}} \propto Pe_D^2$ for small Peclet number, which is consistent with Taylor and Aris analysis [20,21]. The equation also implies the existence of the transition regime from laminar to turbulent, in which we have $k_{dis_{xx}} \propto Pe_D^{1.4}$.

A similar procedure can be taken to estimate the longitudinal thermal dispersion for the case of fully turbulent flow, using the wall laws as

$$u = u_\tau\left(\frac{1}{\kappa}\ln n^+ + B\right) \tag{40}$$

and

$$T - \langle T\rangle^s = -\frac{q_w \sigma_T}{u_\tau \rho_f c_{pf}}\left(\frac{1}{\kappa}\ln n^+ + A\right) \tag{41}$$

where u_τ and q_w are the friction velocity and wall heat flux, respectively, and $n^+ = u_\tau n/v_f$ is the dimensionless distance measured from the wall surface ($n = \frac{H-D}{2} - y$). κ is the von-Karman constant while both B and A are the empirical constants. It is easy to find

$$\tilde{u} = \frac{u_\tau}{\kappa}(\ln\zeta + 1) \tag{42}$$

and

$$\tilde{T} = -\frac{q_w \sigma_T}{u_\tau \rho_f c_{pf}\kappa}(\ln\zeta + 1) \tag{43}$$

where

$$\zeta = 1 - \eta \tag{44}$$

Using these profile functions (42) and (43), we have

$$-\rho_f c_{p_f}\langle \tilde{u}_j\tilde{T}\rangle^f = \frac{\sigma_T q_w}{\kappa^2}\langle(\ln\zeta+1)^2\rangle^f = \frac{\sigma_T q_w}{\kappa^2} = \frac{\sigma_T \rho_f c_{p_f}\langle u\rangle}{\kappa^2 a_f}\frac{\partial\langle T\rangle^f}{\partial x} \tag{45}$$

where we used Eq. (31) to eliminate $q_w = -h_f(\langle T\rangle^f - \langle T\rangle^s)$ in favor of the temperature gradient. Setting κ and σ_T to 0.41 and 0.9, respec-

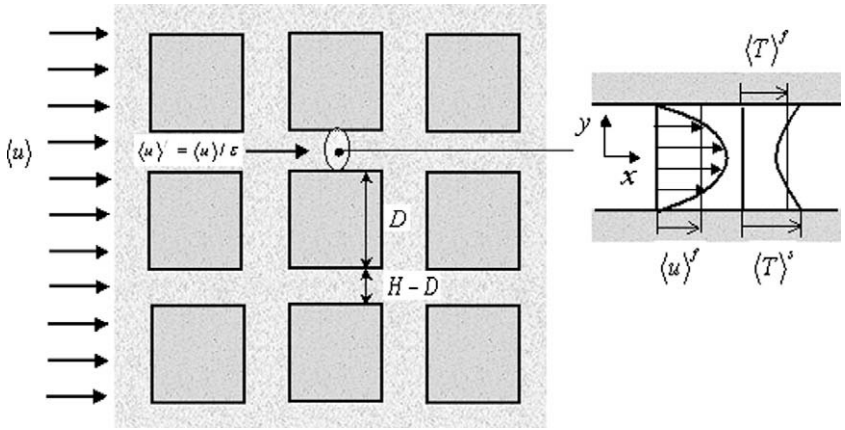

Fig. 8. Cubes in a regular arrangement and prevailing velocity and temperature fields.

tively, according to Launder and Spalding [30], we obtain for the turbulent regime:

$$\frac{k_{dis_{xx}}}{k_f} = \frac{\sigma_T \rho_f c_{p_f} \langle u \rangle}{\kappa^2 a_f k_f} = \frac{\sigma_T}{6(1-\varepsilon)\kappa^2} Pe_D = 1.5 Pe_D : \quad \text{Turbulent regime} \tag{46}$$

Thus, the thermal dispersion conductivity increases in proportion to Peclet number for the turbulent regime. It should be noted that, for the case of turbulent flow, the turbulence thermal conductivity should be added in addition to the thermal dispersion conductivity. However, the recent study of Nakayama and Kuwahara [31] gives $k_{turb}/k_f = 0.0233 Pe_D/(1-\varepsilon)$ for the case of packed beds, which is much smaller than the dispersion thermal conductivity, and thus, can be dropped for the first approximation.

5.2. Transverse thermal dispersion conductivity

The transverse thermal dispersion must be taken into account correctly, when we evaluate the heat transfer from the bounding wall. Let us consider the energy Eq. (26) close enough to the solid surface for the convection to be negligible, but sufficiently away from the solid surface, such that the transverse thermal dispersion dominates over the stagnant thermal diffusion:

$$\varepsilon k_{dis_{yy}} \frac{d^2 \langle T \rangle^f}{dy^2} = a_f h_f (\langle T \rangle^f - \langle T \rangle^s) \tag{47}$$

A magnitude analysis reveals that the convection terms in Eq. (26) vanish near the wall due to no-slip conditions and at the same time that transverse diffusion overwhelms the longitudinal one for $(L/\delta)^2 \sim (L/D)^2 \gg 1$ where δ is the thermal boundary layer thickness. Hence, Eq. (47) may be satisfied for most near wall flow cases. Upon assuming $\langle T \rangle^f = \langle T \rangle^s$ at infinity, we integrate the foregoing equation and obtain

$$\frac{d\langle T \rangle^f}{dy} = -\sqrt{\frac{a_f h_f}{\varepsilon k_{dis_{yy}}}} (\langle T \rangle^f - \langle T \rangle^s) \tag{48}$$

Thus, the transverse thermal dispersion term may be evaluated as follows:

$$\begin{aligned} -\rho_f c_{p_f} \langle \tilde{v} \tilde{T} \rangle^f &= -\rho_f c_{p_f} \langle u \rangle^f (\langle T \rangle^f - \langle T \rangle^s) \langle F(g-1) \rangle^f \\ &= \rho_f c_{p_f} \langle u \rangle^f \sqrt{\frac{\varepsilon k_{dis_{yy}}}{a_f h_f}} \langle F(g-1) \rangle^f \frac{d\langle T \rangle^f}{dy} \end{aligned} \tag{49}$$

Hence,

$$k_{dis_{yy}} = \frac{(\rho_f c_{p_f} \langle u \rangle)^2}{\varepsilon a_f h_f} (\langle F(g-1) \rangle^f)^2 \tag{50}$$

where

$$\tilde{v} = \langle u \rangle^f F(\eta) \tag{51}$$

such that $\langle F \rangle^f = 0$. It is interesting to note that Eq. (50) obtained for the transverse thermal dispersion conductivity is identical to Eq. (33) obtained for the longitudinal thermal dispersion conductivity, except the difference in the multiplicative constants, namely, $(\langle F(g-1) \rangle^f)^2$ and $\langle (f-1)(g-1) \rangle^f$. Fried and Combarnous' experimental data [32] suggest that $\langle (f-1)(g-1) \rangle^f$ is about 20 times larger than $(\langle F(g-1) \rangle^f)^2$ such that we propose the following equations:

$$\frac{k_{dis_{yy}}}{k_f} = 0.0075 \frac{Pe_D^2}{2 + 1.1 Pe_D^{0.6}/Pr^{0.27}} : \quad \text{Laminar regime} \tag{52}$$

$$\frac{k_{dis_{yy}}}{k_f} = 0.075 Pe_D : \quad \text{Turbulent regime} \tag{53}$$

6. Validation of the expressions for longitudinal and transverse thermal dispersion conductivities

In Fig. 9, our results for the case of packed beds are presented in terms of the ratio of the total longitudinal effective thermal conductivity to the fluid thermal conductivity, namely,

$$\frac{k_{total_{xx}}}{k_f} = \frac{k_{stag_{xx}} + \varepsilon k_{dis_{xx}}}{k_f} \tag{54}$$

The present results obtained for the cases of $(Pr,\ k_s/k_f) = (0.71,\ 53.28)$ and $(7.02,\ 2.30)$ are compared with the experimental data reported by Fried and Combarnous [31] and the empirical equation $\varepsilon k_{dis_{xx}}/k_f = 0.5 Pe_D$ proposed by Wakao and Kaguei [18] for high Peclet number. The stagnant thermal conductivity k_{stag} was evaluated using the general Eq. (20a) along with Eqs. (22a) and (22b), which was also added to their experimental data to show the total longitudinal effective thermal conductivity. Fairly good agreement can be seen between the present correlation and the experimental data.

Likewise, the correlations established for the transverse thermal dispersion conductivity are presented along with the experimental data reported by Fried and Combarnous [31] for the transverse thermal dispersion conductivity. The present expressions appear to be in good accord with the experimental data (see Fig. 10).

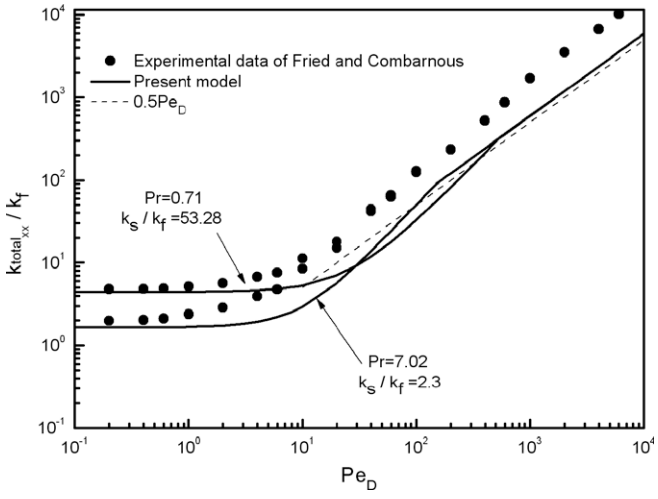

Fig. 9. Longitudinal effective thermal conductivity of packed beds.

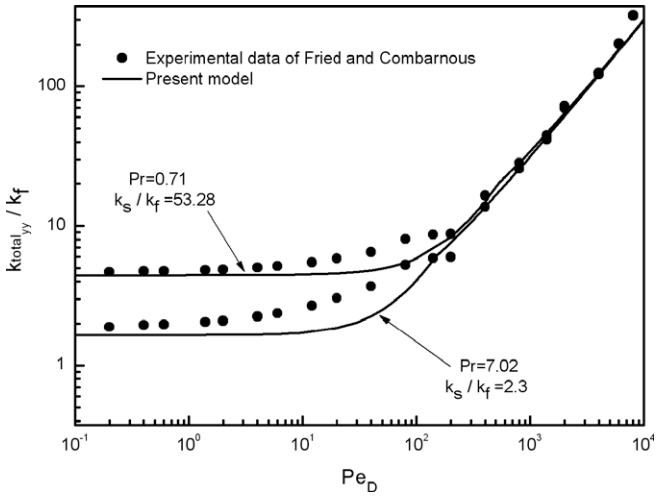

Fig. 10. Transverse effective thermal conductivity of packed beds.

The foregoing comparison suggests that the present expressions for both longitudinal and transverse thermal conductivities are valid for the packed beds. The present expressions as function of the interstitial heat transfer coefficient is quite general, in the sense that they can be applied for other porous media as their correlations for the interstitial heat transfer coefficient are available.

7. Conclusions

A volume averaging theory was exploited to evaluate both stagnant thermal conductivity and thermal dispersion conductivity within porous media. For the stagnant thermal conductivity, a general unit cell model, consisting of rectangular solids with connecting arms in an in-line arrangement, was proposed to describe most homogeneous porous media. The resulting expression for the stagnant thermal conductivity has been validated by comparing the present results with available experimental and theoretical data for packed beds, porous foams and wire screens. As for the thermal dispersion conductivity, a general expression has been derived with help of the two energy equations for solid and fluid phases. It has been revealed that the interfacial heat transfer at the local non-thermal equilibrium controls the spatial distribution of the macroscopic temperature and thus the thermal dispersion activities. The resulting expressions for the longitudinal and transverse thermal dispersion conductivities agree well with available experimental data and empirical correlations.

Acknowledgements

The authors express their sincere thanks to Prof. W. Liu of Huazhong University of Science and Technology for supporting this study. This work has been partially supported by the National Key Basic Research Development Program of China (2007CB 206903).

References

[1] J.C. Maxwell, A Treatise on Electricity and Magnetism, Clarendon Press, Oxford, 1873. p. 365.
[2] L. Rayleigh, On the influence of obstacles arranged in rectangular order upon on the properties of a medium, Philos. Mag. 56 (1892) 481–502.
[3] R.G. Deissler, J.S. Boegli, An investigation of effective thermal conductivities of powders in various gases, ASME Trans. 80 (1958) 1417–1425.
[4] D. Kunii, J.M. Smith, Heat transfer characteristics of porous rocks, AIChE J. 6 (1960) 71–78.
[5] P. Zehner, E.U. Schlunder, Thermal conductivity of granular material at moderate temperatures, Chem. Ing. Tech. 42 (1970) 933–941.
[6] S. Nozad, R.G. Carbonell, S. Whitaker, Heat conduction in multiphase systems, I: theory and experiments for two-phase systems, Chem. Eng. Sci. 40 (1985) 843–855.
[7] M. Sahraouni, M. Kaviany, Slip and non-slip temperature boundary conditions at interface of porous, plain media: conduction, Int. J. Heat Mass Transfer 36 (1993) 1019–1033.
[8] C.T. Hsu, P. Cheng, K.W. Wong, Modified Zehner–Schlunder models for stagnant thermal conductivity of porous media, Int. J. Heat Mass Transfer 37 (1994) 2751–2759.
[9] C.T. Hsu, P. Cheng, K.W. Wong, A lumped parameter model for stagnant thermal conductivity of spatially periodic porous media, ASME Trans. J. Heat Transfer 117 (1995) 264–269.
[10] V.V. Calmid, R.L. Mahajan, The effective thermal conductivity of high porosity fibrous metal foams, ASME Trans. J. Heat Transfer 121 (1999) 466–471.
[11] V.V. Calmid, R.L. Mahajan, Forced convection in high porosity metal foams, ASME Trans. J. Heat Transfer 122 (2000) 557–565.
[12] W.S. Chang, Porosity and effective thermal conductivity of wire screens, ASME Trans. J. Heat Transfer 112 (1990) 5–9.
[13] M. Kaviany, Principles of Heat Transfer in Porous Media, Springer-Verlag, New York, 1991. pp. 115–151.
[14] C.T. Hsu, Heat conduction in porous media, in: K. Vafai (Ed.), Handbook of Porous Media, Marcel Dekker, Inc., New York, 2000, pp. 171–200.
[15] A. Nakayama, PC-Aided Numerical Heat Transfer and Convective Flow, CRC Press, Boca Raton, 1995.
[16] P. Cheng, Heat transfer in geothermal systems, Adv. Heat Transfer 14 (1978) 1–105.
[17] M. Quintard, S. Whitaker, One and two equation models for transient diffusion processes in two-phase systems, Adv. Heat Transfer 23 (1993) 369–465.
[18] N. Wakao, S. Kaguei, Heat and Mass Transfer in Packed Beds, Gordon and Breach, New York, 1996.
[19] S. Yagi, D. Kunii, N. Wakao, Studies on axial effective thermal conductivities in packed beds, AIChE J. 6 (1960) 543–546.
[20] G. Taylor, Dispersion of solute matter in solvent flowing slowly through a tube, Proc. R. Soc. Lond. 15 (1953) 1787–1806.
[21] R. Aris, On the dispersion of a solute in a fluid flowing through a tube, Proc. R. Soc. Lond. 235 (1956) 67–77.
[22] D.L. Koch, J.F. Brady, Dispersion in fixed beds, J. Fluid Mech. 154 (1985) 399–427.
[23] N.W. Han, J. Bhakta, R.G. Carbonell, Longitudinal and lateral dispersion in packed beds: effect of column length and particle size distribution, AIChE J. 31 (1985) 277–288.
[24] D. Vortmeyer, Axial heat dispersion in packed beds, Chem. Eng. Sci. 30 (1975) 999–1001.
[25] F. Kuwahara, A. Nakayama, H. Koyama, A numerical study of thermal dispersion in porous media, Trans. ASME J. Heat Transfer 118 (1996) 756–761.
[26] F. Kuwahara, A. Nakayama, Numerical determination of thermal dispersion coefficients using a periodic porous structure, Trans. ASME J. Heat Transfer 121 (1999) 160–163.
[27] A. Nakayama, F. Kuwahara, Y. Kodama, An equation for thermal dispersion flux transport and its mathematical modelling for heat and fluid flow in a porous medium, J. Fluid Mech. 563 (2006) 81–96.
[28] A. Nakayama, F. Kuwahara, M. Sugiyama, G.L. Xu, A two-energy equation model for conduction and convection in porous media, Int. J. Heat Mass Transfer 44 (2001) 4375–4379.
[29] J.H. VanSant, J.R. Malet, Thermal conductivity of some heat pipe wicks, Lett. Heat Mass Transfer 2 (1975) 199–206.
[30] B.E. Launder, D.B. Spalding, The numerical computation of turbulent flow, Comput. Methods Appl. Mech. Eng. 3 (1974) 269–289.
[31] A. Nakayama, F. Kuwahara, A general macroscopic turbulence model for flows in packed beds, channels, pipes and rod bundles, J. Fluids Eng. 130 (2008). 101205-1–101205-7.
[32] J.J. Fried, M.A. Combarnous, Dispersion in porous media, Adv. Hydrosci. 7 (1971) 169–282.